Acta Pharmacologica Sinica (2012) 33: 407–417

www.nature.com/aps

Original Article

Novel microtubule-targeted agent 6-chloro-4-(methoxyphenyl) coumarin induces G_2-M arrest and apoptosis in HeLa cells

Yi-ming MA, Yu-bo ZHOU*, Chuan-ming XIE, Dong-mei CHEN, Jia LI*

National Center for Drug Screening, State Key Laboratory of Drug Research, Shanghai Institute of Materia Medica, Chinese Academy of Sciences, Shanghai 201203, China

Aim: To identify a novel coumarin analogue with the highest anticancer activity and to further investigate its anticancer mechanisms.
Methods: The viability of cancer cells was investigated using the MTT assay. The cell cycle progression was evaluated using both flow cytometric and Western blotting analysis. Microtubule depolymerization was observed with immunocytochemistry *in vivo* and a tubulin depolymerization assay *in vitro*. Apoptosis was demonstrated using Annexin V/Propidium Iodide (PI) double-staining and sub-G_1 analysis.
Results: Among 36 analogues of coumarin, 6-chloro-4-(methoxyphenyl) coumarin showed the best anticancer activity (IC_{50} value about 200 nmol/L) in HCT116 cells. The compound had a broad spectrum of anticancer activity against 9 cancer cell lines derived from colon cancer, breast cancer, liver cancer, cervical cancer, leukemia, epidermoid cancer with IC_{50} value of 75 nmol/L–1.57 μmol/L but with low cytotocitity against WI-38 human lung fibroblasts (IC_{50} value of 12.128 μmol/L). The compound (0.04–10 μmol/L) induced G_2-M phase arrest in HeLa cells in a dose-dependent manner, which was reversible after the compound was removed. The compound (10–300 μmol/L) induced the depolymerization of purified porcine tubulin *in vitro*. Finally, the compound (0.04–2.5 μmol/L) induced apoptosis of HeLa cells in dose- and time-dependent manners.
Conclusion: 6-Chloro-4-(methoxyphenyl) coumarin is a novel microtubule-targeting agent that induces G_2–M arrest and apoptosis in HeLa cells.

Keywords: anticancer drug; 6-chloro-4-(methoxyphenyl) coumarin; cell cycle arrest; microtubule depolymerization; apoptosis

Acta Pharmacologica Sinica (2012) 33: 407–417; doi: 10.1038/aps.2011.176; published online 23 Jan 2012

Introduction

Coumarins are natural products widely abundant in natural sources, especially green plants. Coumarins have multiple biological activities[1], including anticoagulant[2–4], anti-inflammatory[5, 6], antimicrobial[7–12], antioxidant[13–16], antiallergic[17–20], anti-HIV[21], anticancer[22–28] and antiviral activities[29–32]. It has been suggested that alterations in the chemical structure of coumarins could change their cytotoxic properties. It has also been known for many years that coumarins have significant therapeutic potential[33–35] and are present in many natural therapeutic products[36–40]. Due to their attractive properties and potential clinical utility, we synthesized a series of coumarin analogues and evaluated their anticancer properties to find a novel coumarin analogue with good anticancer activity.

In the present study, we show that 6-chloro-4-(methoxyphenyl) coumarin (CMC) has the best anticancer activity among 36 different coumarin analogues. CMC had broad-spectrum anticancer activities in 9 cancer cell lines derived from 6 different tissues. Further analysis showed that CMC caused G_2-M arrest and apoptosis in HeLa cells via microtubule depolymerization.

Materials and methods

Cell culture

The colon cancer cell line LS-174t was cultured in MEM medium with 10% fetal bovine serum (Hyclone, Thermo Scientific, Logan, UT, USA). The colon cancer cell line HCT-116 was cultured in McCoy's 5A modified medium with 10% fetal bovine serum. The colon cancer cell lines Colo-205 and HCT-15, the breast cancer cell line MDA-MB-435S, and the leukemia cell line HL-60 were cultured in RPMI-1640 with 10% fetal bovine serum. The liver cancer cell line HepG2, the

* To whom correspondence should be addressed.
E-mail jli@mail.shcnc.ac.cn (Jia LI);
ybzhou@mail.shcnc.ac.cn (Yu-bo ZHOU)
Received 2011-09-24 Accepted 2011-11-18

epidermoid cancer cell line A431 and the cervical cancer cell line HeLa were cultured in DMEM (high glucose) with 10% fetal bovine serum. All cell lines mentioned above were purchased from the Cell Bank (Chinese Academy of Sciences, Shanghai, China). A human fetal lung fibroblast cell line (WI-38) was kindly provided by Dr Mei-yu GENG (Shanghai Institute of Materia Medica) and was cultured in MEM with 10% fetal bovine serum (Gibco, Invitrogen, USA). All cells were kept in a humidified atmosphere of 5% CO_2 and 95% air at 37 °C.

Reagents

Coumarin analogues were synthesized and provided by Prof Jie WU from Fudan University. The analogues were dissolved in 100% DMSO with a 5 g/L stock solution. The working solution was prepared by dilution of the stock solution with the culture medium.

An anti-phospho-Ser/Thr-Pro MPM-2 (Cat #05-368) antibody was purchased from Millipore Corporation (Boston, MA, USA). Anti-CDC25C (Cat #4688) antibody was from Cell Signal Technology (Boston, MA, USA). Peroxidase-affiniPure goat anti-rabbit IgG (Code: 112-035-175) and goat anti-mouse IgG (Code: 115-035-174) were purchased from Jackson ImmunoResearch Laboratories, Inc (Baltimore, MD, USA). Hoechst 33342 dye (Cat #H3570) and Alexa Fluor 488 dye-labeled donkey anti-mouse IgG (Cat #A-21202) were purchased from Invitrogen Corporation (Carlsbad, CA, USA).

Cell proliferation assay

The inhibitory effects of synthesized coumarin analogues on the growth of cancer cell lines were evaluated using the MTT viability assay as described previously[41]. Briefly, cells (3000 cells/well) were seeded onto plastic 96-well cell culture plates and cultured at 37 °C. After 24 h, compounds with doses ranging from 10 μmol/L to 10 nmol/L at a dilution ratio of 1:4 were added, and the cells were further incubated for 72 h. MTT was then added to each well at a final concentration of 1 g/L. After a 3 h incubation at 37 °C, the medium was gently discarded and DMSO (100 μL/well) was added to dissolve the formazan product. The optical density was determined at 550 nm/690 nm using a VersaMax Microplate Reader (Molecular Devices). Experiments were performed in four replicates. IC_{50} values were derived from a nonlinear regression model (curvefit) based on a sigmoidal dose response curve (variable slope) and computed using Graphpad Software (Graphpad Prism version 5.02). Data were expressed as the mean±SEM.

Cell cycle analysis

As described previously[42], both synchronized and asynchronized HeLa cells were treated with either DMSO (negative control), nocodazole (positive control), or CMC at 37 °C for the indicated time. The cells were then digested with 0.5 g/L trypsin, collected, washed twice with cold 1×PBS and fixed in 1 mL of 70% ethanol at 4 °C overnight. The next day, cells were washed twice with cold 1×PBS and incubated with 20 μg/mL RNase at 37 °C for 15 min. Cells were then stained with 20 mg/L PI for 30 min at 4 °C. Cell cycle distribution was determined using a BD FACSCalibur Flow Cytometer.

Cell synchronization

HeLa cells were synchronized using a double thymidine block as described previously[43]. Briefly, 1.5×10^5 cells were seeded in each well of a 6-well cell culture plate. The next day, a double thymidine block was performed with an initial block for 17 h and a 10 h release and was followed by a second block for 16 h. The final concentration of thymidine used in the block medium was 2 mmol/L. Following release from the second block, synchronized cells were treated with either DMSO (negative control), nocodazole (positive control) or CMC for the indicated times, and samples were collected for flow cytometry analysis.

Western analysis of G_2-M regulatory proteins

HeLa cells were treated with varying doses of CMC for 24 h. Cells were then lysed with cell lysis buffer [1% NP-40, 150 mmol/L NaCl, 20 mmol/L Tris-HCl, 1 mmol/L EDTA, 1 mmol/L EGTA and complete protease inhibitor cocktail (Cat #11697498001, Roche)]. Equal amounts of protein were resolved by SDS-polyacrylamide gel electrophoresis, transferred onto Hybond-C nitrocellulose membranes (GE Life Sciences) and immunoblotted as described previously[44]. Immunoreactive bands were detected with the enhanced chemiluminescence (ECL) system (GE Life Sciences).

Immunocytochemistry assay

Microtubules were observed using an immunocytochemistry assay[45, 46]. Briefly, HeLa cells were grown on glass coverslips for 24 h and then treated with varying doses of CMC for 8 h. Cells were then fixed with cold methanol (4 °C) for 5 min, blocked for 1 h with 5% BSA in 1×PBS at room temperature and incubated with monoclonal β-tubulin antibody (T-4026; Sigma, St Louis, MO, USA) overnight at 4 °C. Cells were then washed three times with 1×PBS and incubated with Alexa Fluor 488-labeled donkey anti-mouse IgG (Invitrogen) at room temperature for 1 h. The coverslips were washed, stained with 5 mg/L Hoechst 33342 dye (Molecular Probes, Invitrogen) and photographed using an Olympus confocal microscope (Olympus, Tokyo, Japan).

In vitro tubulin polymerization assay

An *in vitro* fluorescence-based tubulin polymerization assay kit (BK011, Cytoskeleton, Inc) was used according to the manufacturer's protocol for monitoring the time-dependent polymerization of tubulin to microtubules. The reaction mixture had a final volume of 50 μL in PEM buffer (80 mmol/L PIPES, 0.5 mmol/L EGTA, 2 mmol/L $MgCl_2$, pH 6.9) and contained 2 g/L bovine brain tubulin, 10 μmol/L fluorescent reporter and 1 mmol/L GTP in either the presence or absence of test compounds at 37 °C. Tubulin polymerization was followed by monitoring fluorescence enhancement due to the incorporation of a fluorescent reporter into microtubules as polymerization proceeded. Fluorescence emission at 450 nm

(excitation wavelength of 360 nm) was measured for 1 h at 0.5 min intervals in a FlexStation 3 Microplate Reader (Molecular Devices). Nocodazole was used as positive control.

Apoptosis detection assay

The quantitative assessment of apoptosis was determined using Annexin V-FITC and PI double staining. Annexin V binds to phosphatidylserine (PS) and other negatively charged phospholipids, thereby producing fluorescence primarily indicative of PS translocation from the inner to the outer cell membrane leaflet. This change reflects aminophospholipid translocase activity in apoptotic cells[47]. PI is a nucleic acid dye that penetrates the nuclear envelope of necrotic cells and was used here as a counterstain to differentiate between live, apoptotic, late-stage apoptotic/early stage necrotic and necrotic cells. Briefly, HeLa cells were treated with varying doses of either CMC or 1 μmol/L stauporine for the indicated times and were then stained with an Annexin V-FITC/PI double staining kit (KGA108, Kaiji Bio Co, Nanjing, China). After washing twice with cold 1×PBS, 5×10^5 cells were collected, resuspended in 500 μL binding buffer with 0.1 g/L Annexin V-FITC and 0.05 g/L PI, and then incubated for 15 min in the dark at room temperature. Finally, the percent of apoptotic cells was immediately measured with a BD FACS Calibur Flow Cytometer and analyzed with CellQuest software (BD Biosciences).

Results

CMC (compound 8) showed the best anticancer activity *in vitro* among the synthesized coumarin analogues

The anticancer activities of different synthesized coumarin analogues were evaluated in HCT116 colon cancer cells using the MTT viability assay. The corresponding chemical structures are shown in Figure 1, and the anticancer activities against HCT116 cells are shown in Table 1. Among the coumarin analogues, CMC (compound **8**) had the best anticancer activity with an IC_{50} value of approximately 200 nmol/L and was selected for further mechanistic study.

Table 1. The *in vitro* anti-proliferation activities of 36 coumarin analogues in HCT116 colorectal carcinoma cells.

Compound ID	IC_{50} (μmol/L)*
1	28.153±2.130
2	1.237±0.159
3	7.809±0.492
4	21.307±1.736
5	33.893±2.764
6	1.661±0.266
7	0.248±0.049
8	0.202±0.038
9	16.297±1.087
10	23.211±1.236
11	28.678±3.109
12	29.303±2.622
13	10.133±1.041
14	34.203±3.131
15	31.893±3.503
16	14.806±1.500
17	10.130±1.120
18	27.552±2.772
19	34.145±3.894
20	3.177±0.200
21	40.520±6.534
22	31.859±3.403
23	16.720±1.653
24	13.440±1.112
25	17.468±0.753
26	13.892±0.576
27	13.897±0.623
28	12.273±0.713
29	12.535±0.631
30	11.548±0.909
31	14.906±0.592
32	9.579±0.441
33	6.896±0.416
34	21.314±0.779
35	22.095±1.536
36	8.183±0.704
doxorubicin	0.061±0.006

*Cell proliferation assay was done according to the method mentioned in the Materials and methods section. The IC_{50} values represent the mean±SEM of quadruplicate determinations.

CMC exhibited very potent anticancer activity against different cancer cell lines

The effect of CMC on the viability of 9 human cancer cell lines derived from 6 different tissues was evaluated using an MTT assay. As shown in Figure 2, CMC exhibited very potent anticancer activity. The IC_{50} values for CMC ranged from 75 nmol/L to 1.57 μmol/L, and the average IC_{50} value was approximately 0.53 μmol/L. Then the selective cytotoxicity of CMC was further evaluated using human normal fetal fibroblast cell line WI-38. CMC exerted markedly weaker cytotoxicity against WI-38 cells with an IC_{50} value of approximately 12.128 μmol/L than against other 9 cancer cell lines.

CMC specifically and reversibly induced G_2-M phase arrest in HeLa cells

Using brightfield microscopy, we found that treatment with CMC caused detachment of adherent cancer cells. The cells became round (data not shown), a phenomenon that occurs during mitosis. To test the possibility that CMC affects mitosis, the effect of CMC on cell cycle progression in HeLa cells was examined. First, HeLa cells were treated with CMC at different concentrations for 24 h. As shown in Figure 3A, CMC treatment resulted in a dose-dependent accumulation of HeLa cells in G_2-M phase with concomitant losses from G_0-G_1 phase. No change in S-phase was observed.

To examine the specificity of the CMC-elicited mitotic arrest, HeLa cells were synchronized at the G_1/S boundary by double thymidine block and were then treated with either 0.63 μmol/L CMC or 0.33 μmol/L nocodazole (positive

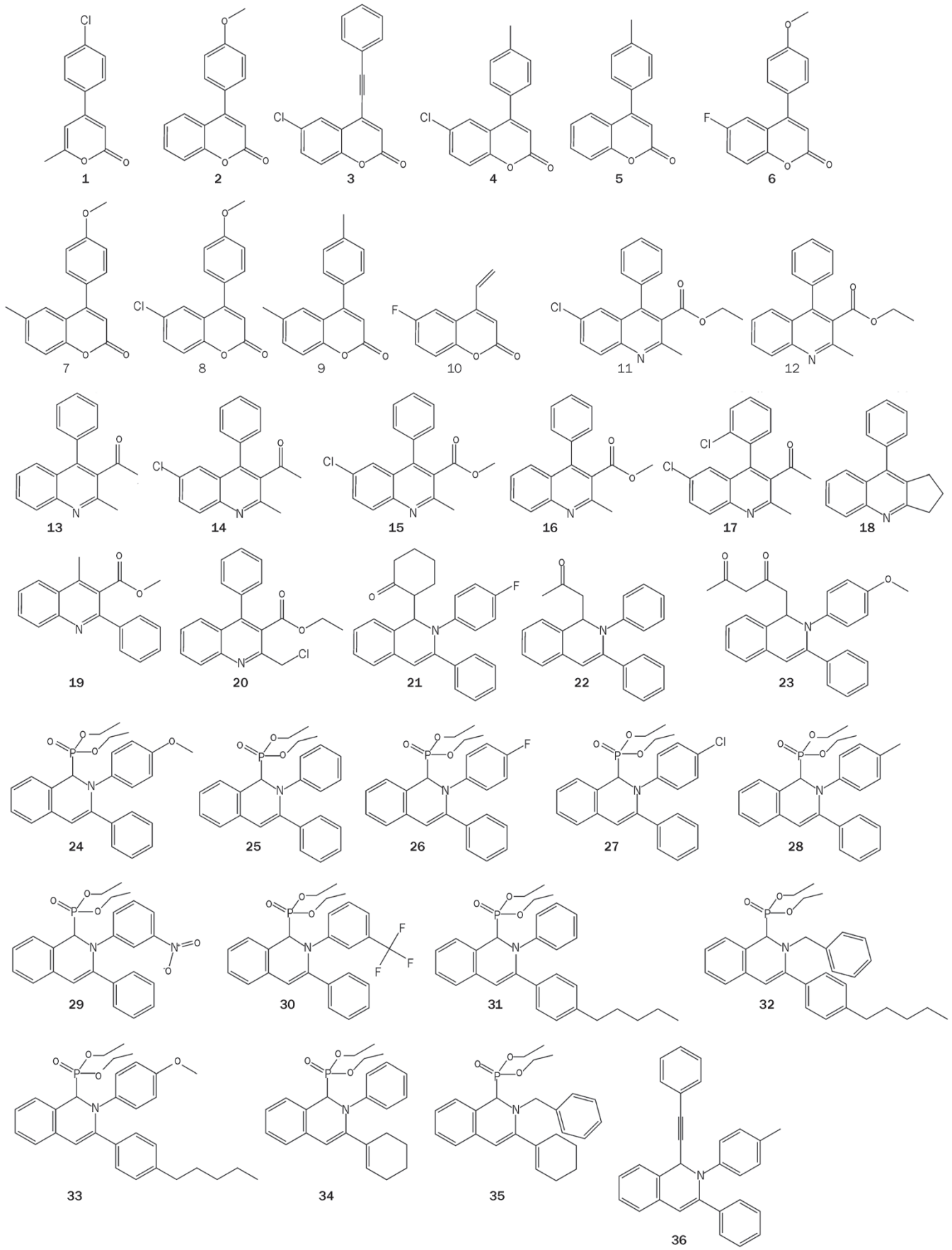

Figure 1. The chemical structures of synthesized coumarin analogues.

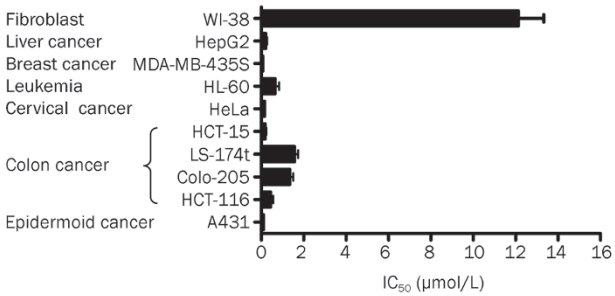

Figure 2. CMC had good anticancer activity in 9 different cancer cell lines. The viability of 9 cancer cell lines and 1 human fetal lung fibroblast cell line was assessed by MTT assay after 72 h of treatment with CMC. All results are expressed as the mean±SEM of four independent experiments.

control) immediately following their release from the block. Flow cytometry analysis was conducted to examine cell cycle progression of CMC-treated cells. Within 6 h and 9 h post-release, CMC-treated cells entered S phase and G_2 phase, respectively, just as did the control cells. However, at the 12 h time point after release, CMC-treated cells were arrested at mitosis in striking contrast to the entrance of control cells into the next cell cycle (Figure 3B). These data indicated that CMC induced an accumulation of cells specifically at G_2-M phase without affecting other cell cycle phases.

Finally, the reversibility of CMC-induced mitotic arrest was assessed by withdrawing CMC immediately after 12 h of treatment. Following CMC withdrawal, arrested cells began to exit from mitosis within 3 h, and 6 h later, most cells entered the next G_1 phase. This result indicated that CMC-induced mitotic arrest is reversible (Figure 3C).

CMC changed the phosphorylation state of G_2-M regulators in HeLa cells

As expected from the previous results, alterations in mitosis-specific protein expression were also detected. Briefly, HeLa cells were treated with CMC at different concentrations for 24 h and then samples were prepared. The levels of MPM-2, CDC25C and β-actin were measured using Western blot analysis. MPM-2 commonly reflects the phosphorylation level of mitosis-specific proteins. As shown in Figure 4, MPM-2 was

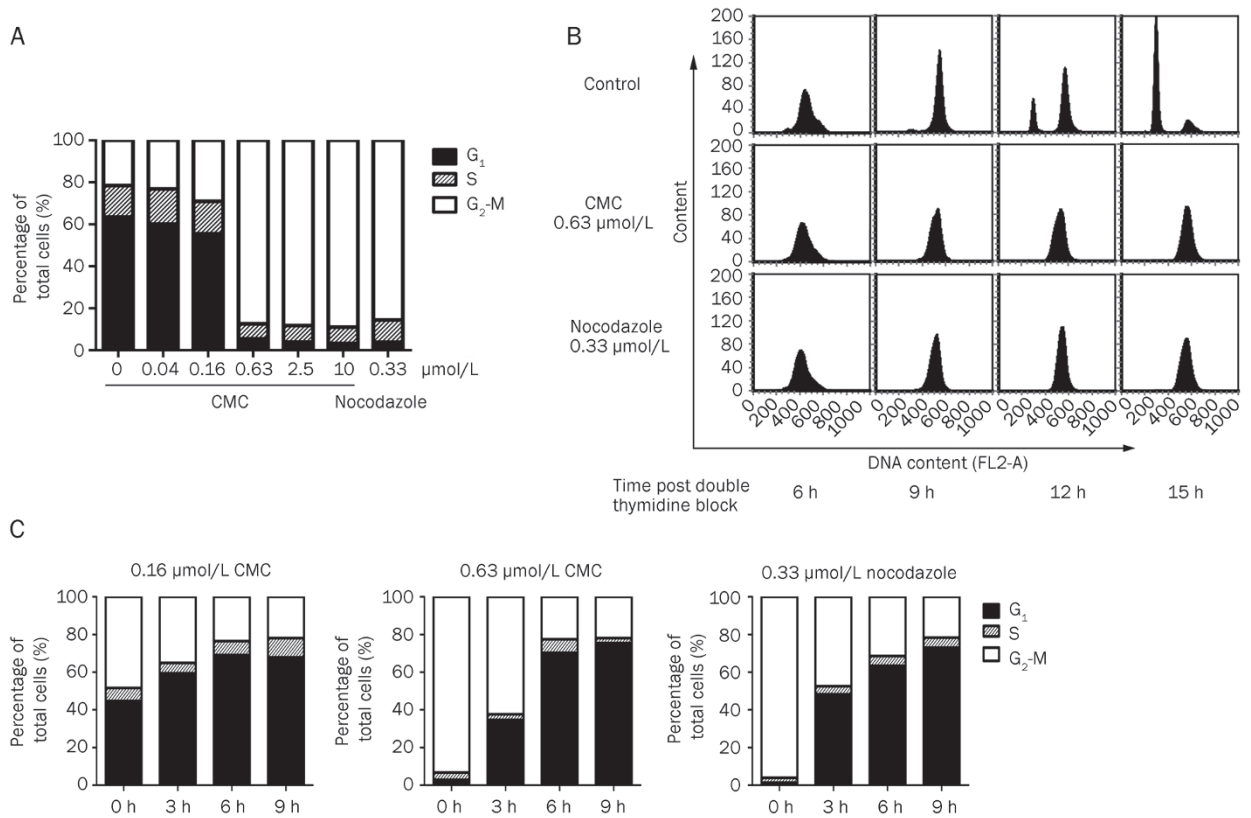

Figure 3. CMC-treated HeLa cells specifically and reversibly arrested in G_2-M phase. (A) HeLa cells arrested in G_2-M phase in a dose-dependent manner. HeLa cells were treated with CMC at doses ranging from 10 μmol/L to 0.04 μmol/L for 24 h. 0.33 μmol/L nocodazole was used as a positive control. The samples were fixed, stained with PI, and analyzed using flow cytometry. (B) HeLa cells were specifically arrested in G_2-M phase. To evaluate if CMC only induced G_2-M arrest, HeLa cells were synchronized at the G_1/S border using a thymidine-thymidine block. The cells were then released and treated with 0.63 μmol/L CMC. Samples were collected at 6 h, 9 h, 12 h, and 15 h and then subjected to flow cytometry analysis. (C) HeLa cells could re-enter the cell cycle following deprivation of CMC. HeLa cells were treated with either CMC or nocodazole (positive control) for 12 h. The medium containing CMC was then removed and fresh medium was added. Samples were collected at 0 h, 3 h, 6 h, and 9 h after deprivation of CMC and then subjected to flow cytometry analysis. All of the data shown are representative of three independent experiments with similar results.

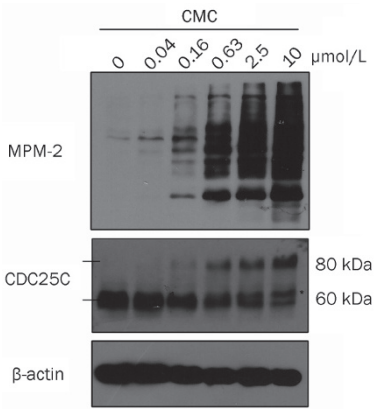

Figure 4. CMC changed the phosphorylation state of G_2-M regulators. HeLa cells were treated with CMC at doses ranging from 10 μmol/L to 0.04 μmol/L for 24 h. 0.1% DMSO was used as a negative control. Phosphorylation of a G_2-M-specific protein (MPM-2) and CDC25C were detected using western blot analysis. β-actin was used as an internal control. MPM-2 and CDC25C antibodies were diluted at 1:1000 in 1×TBST. β-actin antibody was diluted at 1:10000 in 1×TBST. A non-specific band that cross-reacted with the CDC25C antibody is marked with an asterisk.

slightly increased when cells were treated with 0.16 μmol/L CMC but was significantly increased when cells were treated with 0.63 μmol/L CMC. Consistent with this result, there was a shift to a slower migrating form of CDC25C that increased in a dose-dependent manner, which is indicative of changes in the phosphorylation state of the protein. These changes in protein phosphorylation are consistent with cell cycle arrest in mitosis as has been shown previously[48].

CMC induces G_2-M arrest through the depolymerization of microtubules in a direct manner

Cellular microtubules are important components of spindles, which play an important role in mitosis. After sister chromatids are pulled apart by spindles, a single mitotic cell can divide into two cells. To investigate whether CMC affected tubulin polymerization, the microtubule status of CMC-treated HeLa cells was detected by immunocytochemistry. Briefly, cells were exposed to either CMC or a reference drug (nocodazole) for 8 h, fixed and then incubated with β-tubulin antibody at 4 °C overnight. The next day, cells were incubated with Alexa Fluor® 488-labeled donkey anti-mouse IgG, stained with Hoechst 33342 and observed with confocal microscopy.

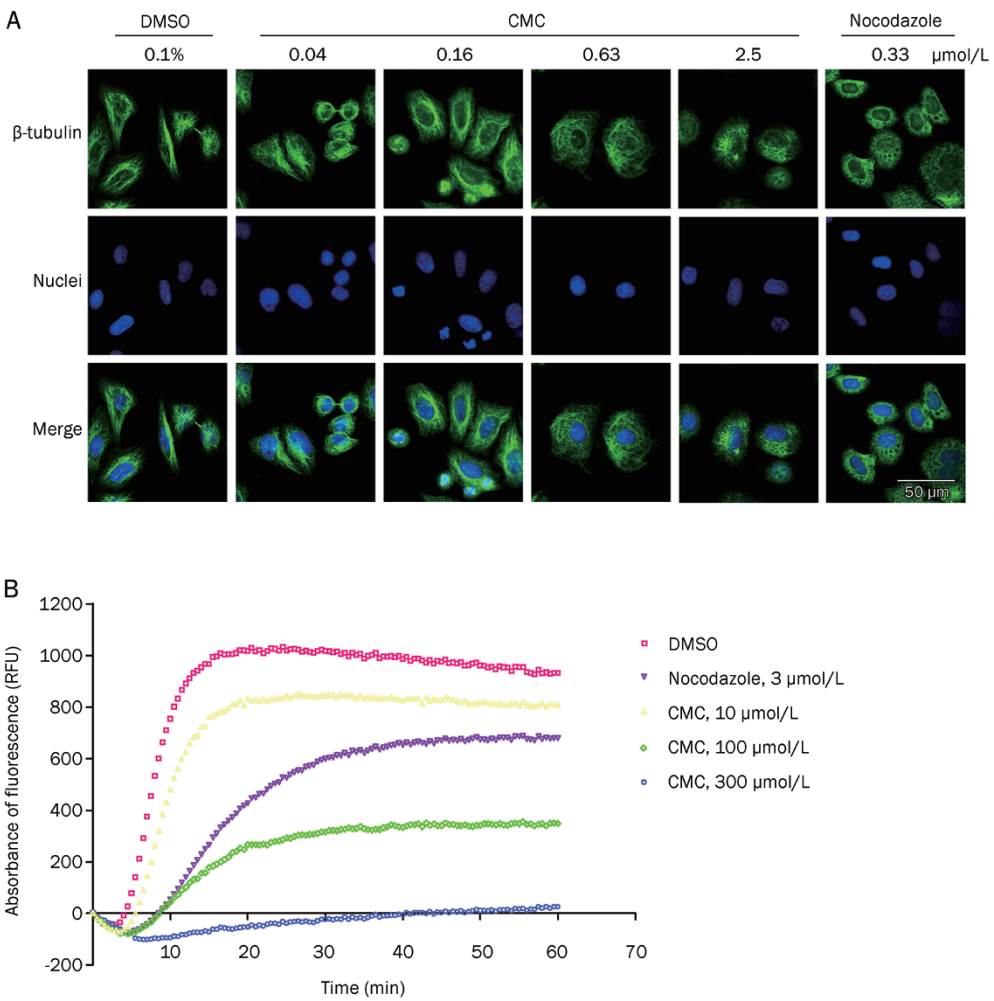

Figure 5. CMC inhibited the polymerization of microtubules. (A) CMC depolymerized microtubules *in vivo*. HeLa cells were treated with CMC at doses ranging from 2.5 μmol/L to 0.04 μmol/L for 8 h. 0.1% DMSO was used as a negative control, and 0.33 μmol/L nocodazole was used as a positive control. Samples were then prepared as mentioned in the "Materials and methods" section, and the status of microtubules was observed using an Olympus confocal microscope (Olym pus, Tokyo, Japan). (B) CMC depolymerized purified tubulin *in vitro*. CMC was added to fluorescently labeled bovine tubulin at 37 °C for 1 h, and its effect on tubulin polymerization was detected with a FlexStation 3 Microplate Reader (Molecular Devices). Nocodazole (3 μmol/L) was used as a positive control, and DMSO was used as a negative control.

CMC depolymerized microtubules in a dose-dependent manner (Figure 5A). When treated with 0.16 μmol/L CMC, the polymerization status of microtubules was only slightly changed; however, when cells were treated with 0.63 μmol/L CMC, almost all microtubules were depolymerized compared with the control group. This phenomenon was consistent with the aforementioned results of the cell cycle and Western blot analyses.

To deduce the mode of CMC-mediated microtubule depolymerization, we used a fluorescence-based tubulin polymerization assay. Nocodazole was used as the positive control. As shown in Figure 5B, CMC inhibited tubulin polymerization in a dose-dependent manner, thereby indicating that CMC inhibited the polymerization of tubulin in a direct manner.

CMC induced apoptosis in a time- and dose-dependent manner

It has been reported that G_2-M arrest caused by microtubule depolymerization is followed by apoptosis[49–51]; therefore, we chose to further investigate the apoptosis induced by CMC.

As shown in Figures 6A and 6B, persistent treatment with CMC led to a progressive increase in apoptosis in a time-dependent manner. Apoptosis of CMC-treated cells increased within 24 h (58.66% viable, 22.09% in early apoptosis and 16.59% cells in late apoptosis). Most cells were apoptotic at 48 h (56.58% in early apoptosis and 29.93% in late apoptosis). At 72 h, most cells were in late apoptosis (17.24% in early apoptosis and 77.87% in late apoptosis).

HeLa cells were then treated with varying doses of CMC for 48 h. As shown in Figures 6C and 6D, the levels of apoptosis in cells treated with 0.04 μmol/L CMC (a dose without induction of G_2-M arrest as shown in Figure 3A) was the same as the negative control. The levels of apoptosis increased in a dose-dependent manner when the cells were treated with G_2-M-arrest-inducing doses (doses greater than 0.16 μmol/L as shown in Figure 3A).

The three-dimensional profile of cell cycle progression *versus* time of CMC treatment shown in Figure 6E demonstrated that G_2-M arrest was maximal (~76.43%) at 12 h of treatment. After this point, the G_2-M population disappeared concomitant with the emergence of a characteristic hypodiploid (<2N DNA) sub-G_1 peak, which indicates apoptotic cells (Figures 6E and 6F). This apoptotic population peaked at 72 h (~59.33%) posttreatment. The *in vitro* findings strongly therefore indicate that CMC-treated cells arrest in G_2-M phase before beginning to apoptose.

Discussion

Coumarins are a hot topic of research due to their diverse pharmaceutical activities and wide distribution in nature. To find a coumarin analogue with good anticancer activity, we synthesized a series of coumarin analogues (Figure 1) and evaluated their effects on the viability of HCT116 cells (Table 1). CMC had the best anticancer activity and was thus selected for further mechanistic study. Nine cancer cell lines derived from 6 different tissues and the WI-38 cell line derived from normal embryonic (3 month gestation) lung tissue were used to evaluate the anticancer effects of CMC. We found that CMC had a high level of anticancer activity *in vitro*, with an IC_{50} value ranging from 75 nmol/L to 1.57 μmol/L. The cytotoxic effect of CMC on WI-38 cells was less potent, with an IC_{50} value of 12.128 μmol/L (Figure 2), which implies that CMC has relative selectivity for cancer cells versus normal cells. CMC also had the best anticancer activity and similar IC_{50} values against the HeLa, MDA-MB-435S, HCT-15, and A431 cell lines. The HeLa cell line was subsequently used for further anticancer mechanism study.

During the above experiments, it came to our attention that CMC caused the evident detachment of HeLa cells that became round (data not shown), a phenomenon frequently observed during the mitotic process. The effect of CMC on cell cycle progression was therefore evaluated to see if CMC affected cellular mitosis. After 24 h of treatment, CMC induced G_2-M arrest in a dose-dependent manner. The minimal dose that caused nearly complete arrest in G_2-M phase was approximately 0.63 μmol/L (Figure 3A); importantly, no concurrent change in S-phase was observed. To determine whether CMC only induced G_2-M arrest, we treated synchronized HeLa cells and found that CMC only influenced G_2-M phase without affecting other cell cycle phases (Figure 3B). G_2-M arrest caused by CMC could be reversed by deprivation of CMC (Figure 3C). Western blot analysis showed that increasing doses of CMC induced increased levels of phosphorylation of G_2-M phase-specific proteins, which provided proof of G_2-M arrest (Figure 4).

When cells were treated with CMC, the cell shape became round with an increased disorder of M-phase-condensed chromosome alignment in a dose-dependent manner (data not shown), which is reported to be induced by alterations to the microtubular cytoskeleton[52]. The microtubule state of CMC-treated cells was therefore tested by ICC. ICC analysis showed that CMC induced microtubule depolymerization after an eight-hour treatment (Figure 5A). Furthermore, CMC effects on tubulin polymerization were tested. These results showed that CMC could inhibit tubulin polymerization directly (Figure 5B). Many articles have reported that G_2-M arrest induced by tubulin-targeting agents is caused by their microtubule depolymerization effects[53–58]. The results shown in Figures 3–5 indicate that CMC caused G_2-M arrest by directly mediating depolymerization of microtubules.

Replicated chromosomes must be accurately segregated into each daughter cell during mitosis, and the spindle checkpoint is a surveillance mechanism that delays anaphase onset until all chromosomes are correctly attached in a bipolar fashion to the mitotic spindle[59]. Chemical inhibition of spindle dynamics, which relieves tension but does not destroy kinetochore-microtubule attachments, activates the spindle checkpoint[60, 61]. From the results shown in Figures 3 and 5, CMC depolymerized microtubules and induced G_2-M arrest in a dose-dependent manner. The dose of CMC needed to depolymerize microtubules is the same as the dose of CMC needed to induce G_2-M arrest, implying that the G_2-M arrest induced by CMC is via microtubule depolymerization.

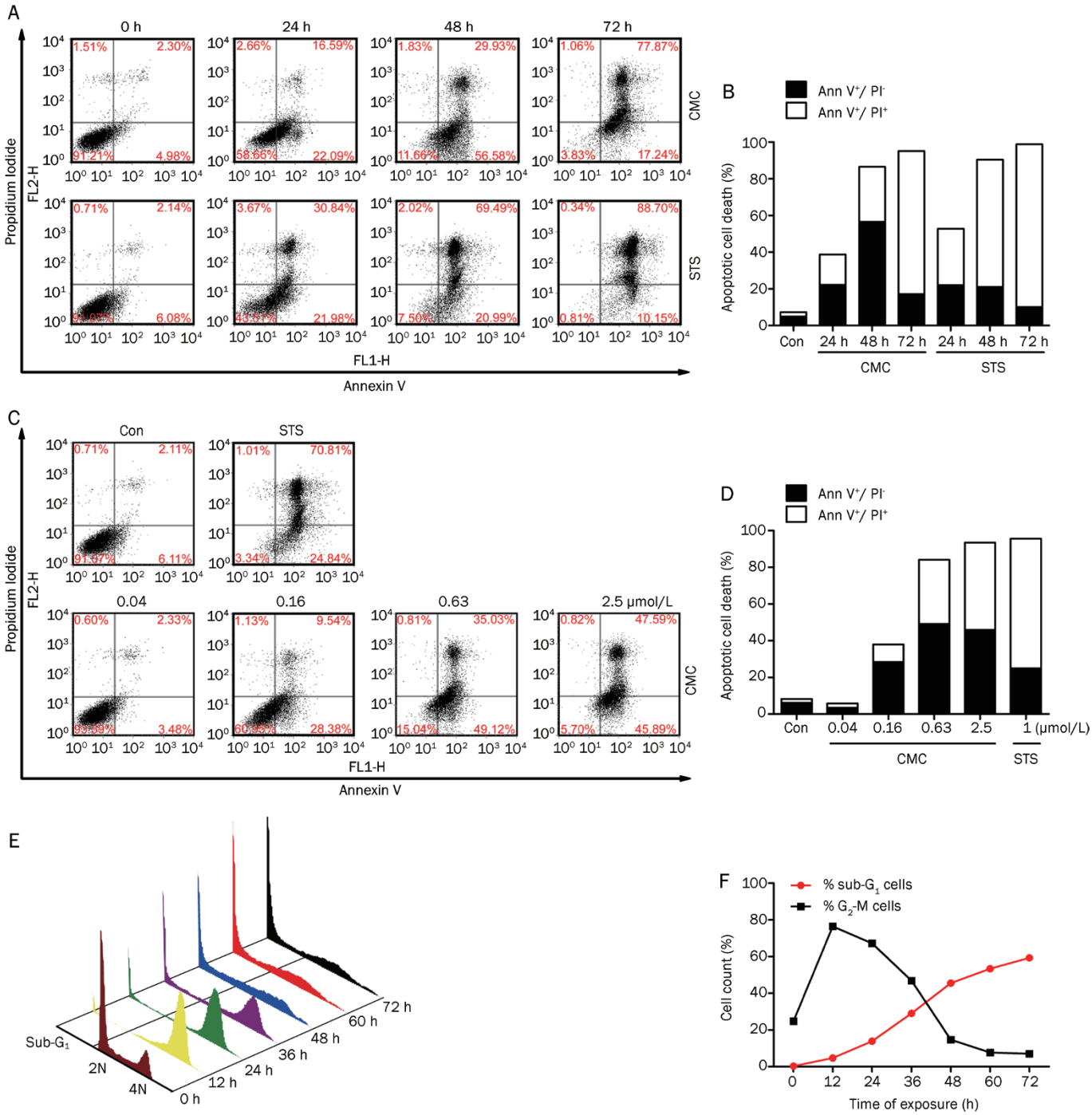

Figure 6. CMC induced apoptosis in a time- and dose-dependent manner. (A) (B) HeLa cells were treated with 0.63 μmol/L CMC. Samples were then collected at 24 h, 48 h, and 72 h followed by staining with Annexin V-FITC/PI. The level of apoptosis was detected using flow cytometry. (C) (D) HeLa cells were treated with CMC at doses ranging from 2.5 μmol/L to 0.04 μmol/L for 48 h. Samples were then stained with Annexin V-FITC/PI. Apoptosis was detected using flow cytometry. (E) (F) HeLa cells were treated with 0.63 μmol/L CMC for 12 h-72 h, and the percentage of sub-G_1 cells and G_2-M cells was analyzed using the ModFit software provided with the FACSCalibur flow cytometer.

It has been reported that microtubule-targeting agents can induce apoptosis via activation of the spindle checkpoint[62]; thus, apoptosis induced by CMC was evaluated using Annexin V/PI double staining. As shown in Figures 6A and 6B, 0.63 μmol/L CMC triggered apoptosis at 24 h and induced apoptosis in a time-dependent manner (Figures 6A and 6B). CMC also caused a significant increase in apoptosis at 48 h in a dose-dependent manner (Figures 6C and 6D), and G_2-M arrest induced by CMC occurs before the commencement of apoptosis (Figures 6E and 6F).

As mentioned, the importance of microtubules in mitosis makes them a superb target for a group of highly successful, chemically diverse anticancer drugs[63–65]. In view of the success of this class of drugs, it has been argued that microtubules represent the best cancer target to be identified so far, and it seems likely that drugs of this class will continue to be important chemotherapeutic agents even as more selective approaches are developed[63–65]. Relatively weak microtubule-targeting coumarins could also be used as adjuvants in chemotherapy to attain increased efficacy with decreased toxicity[63–65]. The maintenance of low concentrations of microtubule-targeted drugs in tumor tissue for long durations could be more efficacious in killing tumor cells than the rapidly rising and falling drug concentrations associated with bolus administration at maximum tolerated doses[63–65]. These advantages make coumarins a hot area for further study.

Still elusive is the fact that different anticancer coumarins with different substitutions can have different mechanisms. It is reported that coumarin can reduce the expression of Ras and Myc, and it can also induce G_0/G_1 arrest and apoptosis via ROS[66]. Another coumarin analogue, decursin, inhibits the proliferation of the advanced human prostate carcinoma cell lines DU145, PC-3 and LNCaP by causing G_1 arrest via an induction of Cip1/p21 and Kip1/p27[22]. Ferulenol and dicoumarol stimulate tubulin assembly[67, 68], and geiparvarin is able to inhibit GTP-induced polymerization[69]. Here, we report on a novel microtubule-targeting coumarin analogue with high anticancer activity. Our results provide clues for structure-activity relationship studies and for further structural design of novel microtubule-targeting coumarin analogues.

Acknowledgements

The authors thank Prof Jie WU from Fudan University for the synthesis of coumarin analogues and Prof Yi CHEN from the Shanghai Institute of Materia Medica for her helpful comments on this work. This work was supported by grants from the National Natural Science Foundation of China (No 30801405 and 81072667).

Author contribution

Yi-ming MA, Yu-bo ZHOU and Jia LI designed the research; Yi-ming MA, Chuan-ming XIE, and Dong-mei CHEN performed the research; Yi-ming MA, Yu-bo ZHOU, and Jia LI analyzed the data; and Yi-ming MA and Yu-bo ZHOU wrote the paper.

References

1 Kumar V, Tomar S, Patel R, Yousaf A, Parmar VS, Malhotra SV. $FeCl_3$-catalyzed Pechmann synthesis of coumarins in Ionic liquids. Synthetic Commun 2008; 38: 2646–54.
2 Mousa SA. Anticoagulants in thrombosis and cancer: the missing link. Expert Rev Anticancer Ther 2002; 2: 227–33.
3 Lowenthal J, Birnbaum H. Vitamin K and coumarin anticoagulants: dependence of anticoagulant effect on inhibition of vitamin K transport. Science 1969; 164: 181–3.
4 Bobek V, Boubelik M, Kovarik J, Taltynov O. Inhibition of adhesion breast cancer cells by anticoagulant drugs and cimetidine. Neoplasma 2003; 50: 148–51.
5 Fylaktakidou KC, Hadjipavlou-Litina DJ, Litinas KE, Nicolaides DN. Natural and synthetic coumarin derivatives with anti-inflammatory/antioxidant activities. Curr Pharm Design 2004; 10: 3813–33.
6 Hadjipavlou-Litina DJ, Litinas KE, Kontogiorgis C. The anti-inflammatory effect of coumarin and its derivatives. Curr Med Chem - Anti-Inflam Anti-Aller Agents 2007; 6: 293–306.
7 Ouahouo BM, Azebaze AG, Meyer M, Bodo B, Fomum ZT, Nkengfack AE. Cytotoxic and antimicrobial coumarins from *Mammea africana*. Ann Trop Med Parasit 2004; 98: 733–9.
8 Creaven BS, Egan DA, Kavanagh K, McCann M, Noble A, Thati B, *et al*. Synthesis, characterization and antimicrobial activity of a series of substituted coumarin-3-carboxylatosilver(I) complexes. Inorg Chim Acta 2006; 359: 3976–84.
9 Widelski J, Popova M, Graikou K, Glowniak K, Chinou I. Coumarins from *Angelica lucida* L–antibacterial activities. Molecules 2009; 14: 2729–34.
10 Vyasa KB, Nimavat KS, Jani GR, Hathi MV. Synthesis and antimicrobial activity of coumarin derivatives metal complexes: an *in vitro* evaluation. Orbital 2009; 1: 183–92.
11 Hishmat OH, Miky JAA, Farrag AA, Fadl-Allah EM. Synthesis of some coumarin derivatives and their antimicrobial activity. Arch Pharm Res 1989; 12: 181–5.
12 Ojala T, Remes S, Haansuu P, Vuorela H, Hiltunen R, Haahtela K, *et al*. Antimicrobial activity of some coumarin containing herbal plants growing in Finland. J Ethnopharmacol 2000; 73: 299–305.
13 Orlov YE. Chemical structure and antioxidant activity among natural coumarins. Chem Nat Comp 1986; 22: 340.
14 Thuong PT, Hung TM, Ngoc TM, Ha DT, Min BS, Kwack SJ, *et al*. Antioxidant activities of coumarins from Korean medicinal plants and their structure-activity relationships. Phytother Res 2010; 24: 101–6.
15 Torres R, Faini F, Modak B, Urbina F, Labbe C, Guerrero J. Antioxidant activity of coumarins and flavonols from the resinous exudate of *Haplopappus multifolius*. Phytochemistry 2006; 67: 984–7.
16 Yu W, Liu ZQ, Liu ZL. Antioxidant effect of coumarin derivatives on free radical initiated and photosensitized peroxidation of linoleic acid in micelles. J Chem Soc, Perkin Trans 1999; 2: 969–74.
17 Simonyan AV, Vlasenko SP, Dimoglo AS. Electron topological study of the link between antiallergic activity and structure for chalcone, coumarin and cinnamic acid derivatives. Pharm Chem J 1993; 27: 490–4.
18 Nugroho AE, Riyanto S, Sukari MA, Maeyama K. Anti-allergic effects of Marmin, a coumarine isolated from *Aegle marmelos* Correa: *In vitro* study. Int J Phytomed 2011; 3: 84–97.
19 Gonsior E, Schultze-Werninghaus G, Wuthrich B. Protective anti-allergic effects of a new coumarin compound (BM 15.100) in experimental asthma. Int J Clin Pharmacol Biopharm 1979; 17: 283–9.
20 Matsuda H, Tomohiro N, Ido Y, Kubo M. Anti-allergic effects of cnidii monnieri fructus (dried fruits of *Cnidium monnieri*) and its major component, osthol. Biol Pharmaceut Bull 2002; 25: 809–12.
21 Buckle DR, Outred DJ, Smith H, Spicer BA. N-benzylpiperazino derivatives of 3-nitro-4-hydroxycoumarin with H1 antihistamine and mast cell stabilizing properties. J Med Chem 1984; 27: 1452–7.
22 Yim D, Singh RP, Agarwal C, Lee S, Chi H, Agarwal R. A novel anticancer agent, decursin, induces G_1 arrest and apoptosis in human prostate carcinoma cells. Cancer Res 2005; 65: 1035–44.
23 Belluti F, Fontana G, Dal Bo L, Carenini N, Giommarelli C, Zunino F. Design, synthesis and anticancer activities of stilbene-coumarin hybrid compounds: Identification of novel proapoptotic agents. Bioorg Med Chem 2010; 18: 3543–50.
24 Kamal A, Adil SF, Tamboli, Jaki R, Siddardha B, Murthy USN. Synthesis

of coumarin linked naphthalimide conjugates as potential anticancer and antimicrobial agents. Lett Drug Design Disc 2009; 6: 201–9.
25 Kawase M, Sakagami H, Motohashi N, Hauer H, Chatterjee SS, Spengler G, *et al*. Coumarin derivatives with tumor-specific cytotoxicity and multidrug resistance reversal activity. *In Vivo* 2005; 19: 705–11.
26 Reddy NS, Mallireddigari MR, Cosenza S, Gumireddy K, Bell SC, Reddy EP, *et al*. Synthesis of new coumarin 3-(N-aryl) sulfonamides and their anticancer activity. Bioorg Med Chem Lett 2004; 14: 4093–7.
27 Bhattacharyya SS, Paul S, Mandal SK, Banerjee A, Boujedaini N, Khuda-Bukhsh AR. A synthetic coumarin (4-methyl-7 hydroxy coumarin) has anti-cancer potentials against DMBA-induced skin cancer in mice. Eur J Pharm 2009; 614: 128–36.
28 Devji T, Reddy C, Woo C, Awale S, Kadota S, Carrico-Moniz D. Pancreatic anticancer activity of a novel geranylgeranylated coumarin derivative. Bioorg Med Chem Lett 2011; 21: 5770–3.
29 Ishikawa T, Kotake K, Ishii H. Synthesis of toddacoumaquinone, a coumarin-naphthoquinone dimer, and its antiviral activities. Chem Pharm Bull 1995; 43: 1039–41.
30 Hwu JR, Singha R, Hong SC, Chang YH, Das AR, Vliegen I, *et al*. Synthesis of new benzimidazole-coumarin conjugates as anti-hepatitis C virus agents. Antiviral Res 2008; 77: 157–62.
31 Yang Z, Xiao H, Liu Y, Liu J, Wen L. Antiviral effect of coumarin analogue against respiratory syncytical virus infection *in vitro* and *in vivo*. Antiviral Res 1995; 26: 350–350.
32 Curini M, Epifano F, Maltese F, Marcotullio MC, Gonzales SP, Rodriguez JC. Synthesis of collinin, an antiviral coumarin. Aust J Chem 2003; 56: 59–60.
33 Hoult JR, Payá M. Pharmacological and biochemical actions of simple coumarins: natural products with therapeutic potential. Gen Pharmacol 1996; 27: 713–22.
34 Oldenburg J, Seidel H, Potzsch B, Watzka M. New insight in therapeutic anticoagulation by Coumarin derivatives. Hamostaseologie 2008; 28: 44–50.
35 Riveiro ME, De Kimpe N, Moglioni A, Vázquez R, Monczor F, Shayo C, *et al*. Coumarins: old compounds with novel promising therapeutic perspectives. Curr Med Chem 2010; 17: 1325–38.
36 Enderle C, Müller W, Grass U. Drug interaction: omeprazole and phenprocoumon. BMC Gastroenterol 2001; 1: 2.
37 Holbrook AM, Pereira JA, Labiris R, McDonald H, Douketis JD, Crowther M, *et al*. Systematic overview of warfarin and its drug and food interactions. Arch Intern Med 2005; 165: 1095–106.
38 Irena K. Studying plant-derived coumarins for their pharmacological and therapeutic properties as potential anticancer drugs. Expert Opin Drug Disc 2007; 2: 1605–18.
39 Montes R, Ruiz de Gaona E, Martinez-González MA, Alberca I, Hermida J. The c.-1639G > A polymorphism of the VKORC1 gene is a major determinant of the response to acenocoumarol in anticoagulated patients. Br J Haematol 2006; 133: 183–7.
40 Thornes RD, Lynch G, Sheehan MV. Cimetidine and coumarin therapy of melanoma. Lancet 1982; 2: 328.
41 Zang Y, Yu LF, Pang T, Fang LP, Feng X, Wen TQ, *et al*. AICAR induces astroglial differentiation of neural stem cells via activating the JAK/STAT3 pathway independently of AMP-activated protein kinase. J Biol Chem 2008; 283: 6201–8.
42 Zang Y, Yu LF, Nan FJ, Feng LY, Li J. AMP-activated protein kinase is involved in neural stem cell growth suppression and cell cycle arrest by 5-aminoimidazole-4-carboxamide-1-beta-D-ribofuranoside and glucose deprivation by down-regulating phospho-retinoblastoma protein and cyclin D. J Biol Chem 2009; 284: 6175–84.
43 Bengoechea-Alonso MT, Punga T, Ericsson J. Hyperphosphorylation regulates the activity of SREBP1 during mitosis. Proc natl Acad Sci U S A 2005; 102: 11681–6.
44 Zhou YB, Feng X, Wang LN, Du JQ, Zhou YY, Yu HP, *et al*. LGH00031, a novel ortho-quinonoid inhibitor of cell division cycle 25B, inhibits human cancer cells via ROS generation. Acta Pharmacol Sin 2009; 30: 1359–68.
45 Mooberry SL, Tien G, Hernandez AH, Plubrukarn A, Davidson BS. Laulimalide and isolaulimalide, new paclitaxel-like microtubule-stabilizing agents. Cancer Res 1999; 59: 653–60.
46 Sherr CJ. Cancer cell cycles. Science 1996; 274: 1672–7.
47 Bratton DL, Fadok VA, Richter DA, Kailey JM, Guthrie LA, Henson PM. Appearance of phosphatidylserine on apoptotic cells requires calcium-mediated nonspecific flip-flop and is enhanced by loss of the aminophospholipid translocase. J Biol Chem 1997; 272: 26159–65.
48 Scatena CD, Stewart ZA, Mays D, Tang LJ, Keefer CJ, Leach SD, *et al*. Mitotic phosphorylation of Bcl-2 during normal cell cycle progression and Taxol-induced growth arrest. J Biol Chem 1998; 273: 30777–84.
49 Aneja R, Liu M, Yates C, Gao J, Dong X, Zhou B, *et al*. Multidrug resistance-associated protein-overexpressing teniposide-resistant human lymphomas undergo apoptosis by a tubulin-binding agent. Cancer Res 2008; 68: 1495–503.
50 Hwang JH, Takagi M, Murakami H, Sekido Y, Shin-ya K. Induction of tubulin polymerization and apoptosis in malignant mesothelioma cells by a new compound JBIR-23. Cancer Lett 2011; 300: 189–96.
51 Chakrabarty S, Das A, Bhattacharya A, Chakrabarti G. Theaflavins depolymerize microtubule network through tubulin binding and cause apoptosis of cervical carcinoma HeLa cells. J Agr Food Chem 2011; 59: 2040–8.
52 Eichenlaub-Ritter U, Chandley AC, Gosden RG. Alterations to the microtubular cytoskeleton and increased disorder of chromosome alignment in spontaneously ovulated mouse oocytes aged *in vivo*: an immunofluorescence study. Chromosoma 1986; 94: 337–45.
53 Loganzo F, Discafani CM, Annable T, Beyer C, Musto S, Hari M, *et al*. HTI-286, a synthetic analogue of the tripeptide hemiasterlin, is a potent antimicrotubule agent that circumvents P-glycoprotein-mediated resistance *in vitro* and *in vivo*. Cancer Res 2003; 63: 1838–45.
54 Bacher G, Nickel B, Emig P, Vanhoefer U, Seeber S, Shandra A, *et al*. D-24851, a novel synthetic microtubule inhibitor, exerts curative antitumoral activity *in vivo*, shows efficacy toward multidrug-resistant tumor cells, and lacks neurotoxicity. Cancer Res 2001; 61: 392–9.
55 Zhang LH, Wu L, Raymon HK, Chen RS, Corral L, Shirley MA, *et al*. The synthetic compound CC-5079 is a potent inhibitor of tubulin polymerization and tumor necrosis factor-alpha production with antitumor activity. Cancer Res 2006; 66: 951–9.
56 Towle MJ, Salvato KA, Budrow J, Wels BF, Kuznetsov G, Aalfs KK, *et al*. *In vitro* and *in vivo* anticancer activities of synthetic macrocyclic ketone analogues of halichondrin B. Cancer Res 2001; 61: 1013–21.
57 Kasibhatla S, Baichwal V, Cai SX, Roth B, Skvortsova I, Skvortsov S, *et al*. MPC-6827: a small-molecule inhibitor of microtubule formation that is not a substrate for multidrug resistance pumps. Cancer Res 2007; 67: 5865–71.
58 Tahir SK, Han EK, Credo B, Jae HS, Pietenpol JA, Scatena CD, *et al*. A-204197, a new tubulin-binding agent with antimitotic activity in tumor cell lines resistant to known microtubule inhibitors. Cancer Res 2001; 61: 5480–5.
59 May KM, Hardwick KG. The spindle checkpoint. J Cell Sci 2006; 119: 4139–42.
60 Clute P, Pines J. Temporal and spatial control of cyclin B1 destruction in metaphase. Nat Cell Biol 1999; 1: 82–7.
61 Nicklas RB, Waters JC, Salmon ED, Ward SC. Checkpoint signals in grasshopper meiosis are sensitive to microtubule attachment, but

tension is still essential. J Cell Sci 2001; 114: 4173–83.
62 Carré M, Braguer D. Microtubule damaging agents and apoptosis. In: Tito Fojo Editor. The role of microtubules in cell biology, neurobiology and oncology. Humana Press; 2008. p 479–518.
63 Jordan MA, Wilson L. Microtubules as a target for anticancer drugs. Nature Reviews 2004; 4: 253–65.
64 Hadfield JA, Ducki S, Hirst N, McGown AT. Tubulin and microtubules as targets for anticancer drugs. Prog Cell Cycle Res 2003; 5: 309–25.
65 Jordan MA, Kamath K. How do microtubule-targeted drugs work? An overview. Curr Cancer Drug Tar 2007; 7: 730–42.
66 Chuang JY, Huang YF, Lu HF, Ho HC, Yang JS, Li TM, *et al*. Coumarin induces cell cycle arrest and apoptosis in human cervical cancer HeLa cells through a mitochondria- and caspase-3 dependent mechanism and NF-kappaB down-regulation. *In Vivo* 2007; 21: 1003–9.
67 Bocca C, Gabriel L, Bozzo F, Miglietta A. Microtubule-interacting activity and cytotoxicity of the prenylated coumarin ferulenol. Planta Med 2002; 68: 1135–7.
68 Madari H, Panda D, Wilson L, Jacobs RS. Dicoumarol: a unique microtubule stabilizing natural product that is synergistic with Taxol. Cancer Res 2003; 63: 1214–20.
69 Miglietta A, Bocca C, Gabriel L, Rampa A, Bisi A, Valenti P. Anti-microtubular and cytotoxic activity of geiparvarin analogues, alone and in combination with paclitaxel. Cell Biochem Funct 2001; 19: 181–9.